From 1-D Coordination Polymers to 3-D Hydrogen-Bonding Networks: Crystal Engineering and Magnetism of CuII−dca −Cyanopyridine Supramolecular Systems (dca = Dicyanamide, N(CN)2-)†

ARTICLE *in* CRYSTAL GROWTH & DESIGN · DECEMBER 2004

Impact Factor: 4.89 · DOI: 10.1021/cg0496888

4 AUTHORS:

Miao Du
Tianjin Normal University
307 PUBLICATIONS **9,097** CITATIONS
SEE PROFILE

Xiao-Jun Zhao
Tianjin Normal University
170 PUBLICATIONS **3,808** CITATIONS
SEE PROFILE

Stuart R. Batten
Monash University (Australia)
311 PUBLICATIONS **14,498** CITATIONS
SEE PROFILE

Joan Ribas
374 PUBLICATIONS **11,901** CITATIONS
SEE PROFILE

CRYSTAL GROWTH & DESIGN
2005
VOL. 5, NO. 3
901−909

From 1-D Coordination Polymers to 3-D Hydrogen-Bonding Networks: Crystal Engineering and Magnetism of Cu^{II}−dca−Cyanopyridine Supramolecular Systems (dca = Dicyanamide, $N(CN)_2^-$)†

Miao Du,*,‡ Xiao-Jun Zhao,‡ Stuart R. Batten,§ and Joan Ribas||

College of Chemistry and Life Science, Tianjin Normal University, Tianjin 300074, People's Republic of China, School of Chemistry, P.O. Box 23, Monash University, Clayton, Victoria, 3800, Australia, and Departament de Química Inorgànica, Universitat de Barcelona, Diagonal, 647, 08028-Barcelona, Spain

Received September 9, 2004; Revised Manuscript Received October 19, 2004

Ⓦ **This paper contains enhanced objects available on the Internet at http://pubs.acs.org/crystal.**

ABSTRACT: Three-dimensional (3-D) metallo-supramolecular architectures **1**−**3** based on Cu^{II}−dca−cypy systems [dca = dicyanamide, $N(CN)_2^-$, and cypy = *n*-cyanopyridine (*n* = 4, 3, 2)], which are extended by combining metal-coordination and second-sphere hydrogen-bonded interactions, were rationally designed and structurally characterized by single-crystal X-ray diffraction. Reaction of Cu^{II} with dca and 4- or 3-cypy afforded two similar neutral one-dimensional (1-D) coordination polymers, $[Cu(dca)_2(4\text{-cypy})_2]_n$ (**1**) and $[Cu(dca)_2(3\text{-cypy})_2]_n$ (**2**), in which the octahedral Cu^{II} centers are linked through double $\mu_{1,5}$-dca bridges and the cypy moieties act as monodentate terminal ligands via their pyridyl nitrogen donors. The coordination chains of **1** and **2** are further cross-linked by C−H···N interactions between the free nitrile N atoms of cypy and H atoms of the pyridyl ring, creating two interpenetrating 3-D networks (for **2**, further weaker hydrogen-bonding interactions between the amide N atoms of dca and the H atoms in 3-cypy combined the two networks into a single net). When substituting the 4- or 3-cypy with 2-cypy, a single $\mu_{1,5}$-dca bridged 1-D chain $[Cu(dca)_2(pyom)]_n$ (**3**) was isolated in which the square-pyramidal Cu^{II} center is chelated to the ligand *O*-methyl picolinimidate (pyom), generated from 2-cypy via addition of methanol across the C≡N group. These 1-D chains are further cross-linked by weak $Cu-N_{dca}$ interactions to form corrugated 2-D (6,3) sheets, which are highly interdigitated and further expanded to result in a 3-D network through interlayer C(N)−H···N interactions. Variable-temperature magnetic susceptibility measurements reveal the existence of very weak antiferromagnetic or nil interactions between the Cu^{II} centers in complexes **1**−**3**, and the magneto-structural correlations of such $\mu_{1,5}$-dca−Cu^{II} 1-D systems are also discussed.

Introduction

The realm of crystal engineering is of growing interest, and great efforts have been devoted to the assembly of supramolecular systems of organic molecular solids and coordination polymers through hydrogen bonds and/or coordination bonds, with the resultant crystalline materials having a wide range of potential applications.[1−4] Recently, coordination polymers of dicyanamide anion, $N(CN)_2^-$ (dca), have become a hot topic in this field as a new class of magnetic materials, especially in the form of the binary α-$[M(dca)_2]_n$ materials, which exhibit three-dimensional (3-D) rutile-type topology and interesting long-range ferromagnetic (M = Co^{II}, Ni^{II}, Cu^{II}) or canted spin antiferromagnetic (M = Cr^{II}, Mn^{II}, Fe^{II}) ordering.[5] Of further importance, from a structural perspective, dca is also a remarkable building block for the construction of various functional coordination architectures, such as discrete mononuclear and dinuclear molecular compounds,[6] as well as one-dimensional (1-D) chains, tubes, or ladders, two-dimensional (2-D) (4,4) or (6,3) sheets, and 3-D supramolecular networks, when terminal or bridging coligands (L) are introduced to form M^{II}−dca−L ternary systems and thus modify the properties of these new materials. This attests to the coordinative versatility of dca (a total of eight coordination modes have been observed so far, including monodentate, bidentate, tridentate, and even tetradentate and pentadentate modes; see Chart 1).[7]

One of the best strategies for the construction of high-dimensional supramolecular systems is to utilize second-sphere interactions, such as hydrogen bonds, between the coordinatively unsaturated complexes.[8] Although a useful way to realize this strategy is to extend the 1-D coordination polymers via the hydrogen-bonded interactions, networks designed in this way are still quite rare and are often assembled through hydrogen bonds between lattice/coordinated water and/or anions, and not the 1-D system itself.[9] In this work, we chose *n*-cyanopyridines (cypy, *n* = 4, 3, 2) as the auxiliary ligands of the M^{II}−dca systems to realize this rational engineering considering the following points: these bidentate ligands contain two types of nitrogen donors with the donor ends differing in steric requirements and basic character, the cyano-nitrogen atom being perhaps a much weaker donor than the pyridyl-nitrogen donor when coordinating to the transition metal ions.[10] Consequently, the dca anions and pyridyl-nitrogen donor

† Dedicated to Professor Gui-Lin Wang on the occasion of his 60th birthday.

* To whom correspondence should be addressed. Fax & Tel: 86-22-23540315. E-mail: dumiao@public.tpt.tj.cn.
‡ Tianjin Normal University.
§ Monash University.
|| Universitat de Barcelona.

10.1021/cg0496888 CCC: $30.25
Published on Web 12/08/2004

Chart 1

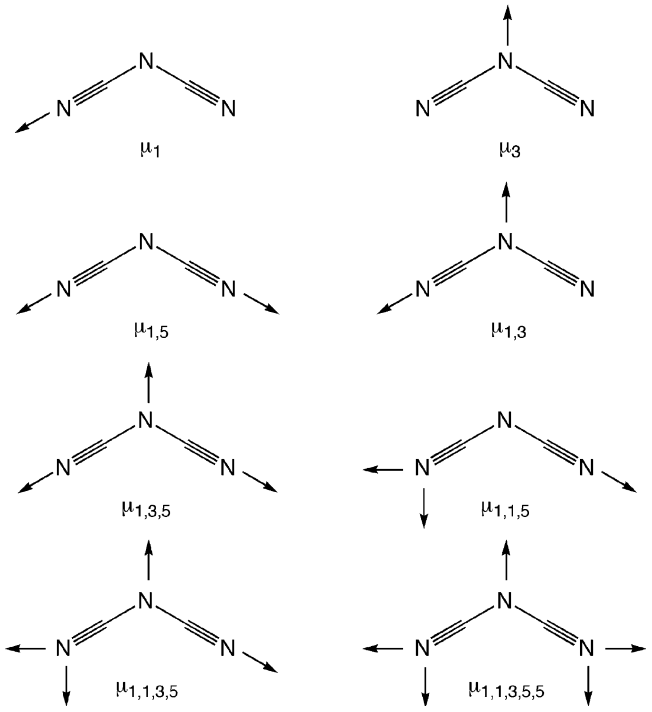

are anticipated to bind to the Cu^{II} center more easily than the cyano-nitrogen atom, resulting in coordination compounds in which the *n*-cypy act only as monodentate ligands and the cyano groups are not involved in metal coordination. For such M^{II}−dca−L systems (L referring to terminal coligand), 1-D structures extended by single or double $\mu_{1,5}$-dca bridges are usually observed, and only a small number of 2-D (6,3) or (4,4) sheets and two 3-D networks have been reported, according to a recent review by Batten and Murray.[7] Thus, the free cyano-nitrogen atoms may act as the acceptors of the interchain C−H···N interactions, further generating supramolecular patterns with higher dimensionality. In this contribution, we will describe the crystal engineering of this design, including the molecular and supramolecular structures of 1-D coordination polymers $[Cu(dca)_2(4\text{-cypy})_2]_n$ (**1**), $[Cu(dca)_2(3\text{-cypy})_2]_n$ (**2**), and $[Cu(dca)_2(pyom)]_n$ (**3**). The reaction of 2-cypy and Cu^{II} in methanol leads to the formation of a chelate ligand *O*-methyl picolinimidate (pyom). On the other hand, the evaluation of the exchange coupling through dca is quite complicated due to the lack of a theoretical model to analyze the magnetic properties of the high-dimensional metal compounds, and thus 1-D Cu^{II}−dca systems are clearly the best examples to characterize the ability of the dca anion to mediate the magnetic interactions. Therefore, the magnetic properties of complexes **1**−**3** were investigated, and the magneto-structural correlations were analyzed.

Experimental Section

Materials and Physical Measurement. All the starting materials and solvents for syntheses were obtained commercially and used as received. FT-IR spectra (KBr pellets) were taken on an AVATAR-370 (Nicolet) spectrometer. Carbon, hydrogen, and nitrogen analyses were performed on a CE-440 (Leemanlabs) analyzer. Thermal stability (thermogravimetric analysis, TGA) experiment was carried out on a Dupont thermal analyzer from room temperature to 900 °C under a nitrogen atmosphere at a heating rate of 10 °C/min.

Magnetic Studies. The variable-temperature magnetic susceptibilities were measured in "Servei de Magnetoquímica (Universitat de Barcelona)" on polycrystalline samples (30 mg) with a Quantum Design MPMS SQUID susceptometer operating at a magnetic field of 0.1 T between 2 and 300 K. The diamagnetic corrections were evaluated from Pascal's constants for all the constituent atoms. Electron spin resonance (ESR) spectra were recorded on powder samples at X-band frequency with a Bruker 300E automatic spectrometer, varying the temperature between 4 and 298 K.

Synthesis of $[Cu(dca)_2(4\text{-cypy})_2]_n$ (1). 4-Cyanopyridine (54 mg, 0.5 mmol) and sodium dicyanamide (45 mg, 0.5 mmol) were dissolved in a CH_3OH/H_2O mixture (30 mL). To the above solution was added a dilute aqueous solution (10 mL) of $Cu(ClO_4)_2\cdot 6H_2O$ (75 mg, 0.2 mmol) under stirring, and a small amount of blue precipitate was observed, which was dissolved after adding additional water (10 mL). The resultant clear solution was filtered and left to stand at room temperature. Light-blue prisms suitable for X-ray diffraction were obtained by slow evaporation of the solvents within 2 weeks in 80% yield. Anal. Calcd for $C_{16}H_8CuN_{10}$: C, 47.59; H, 2.00; N, 34.68%. Found: C, 47.84; H, 2.21; N, 34.75%. IR (cm^{-1}): 3051*m*, 3013*m*, 2290*vs*, 2244*vs*, 2176*vs*, 1611*s*, 1549*m*, 1497*m*, 1421*vs*, 1332*s*, 1225*s*, 1067*m*, 1028*m*, 970*w*, 942*m*, 879*m*, 834*s*, 798*m*, 781*m*, 733*m*, 680*m*, 626*w*, 561*s*, 527*s*, 500*s*.

Synthesis of $[Cu(dca)_2(3\text{-cypy})_2]_n$ (2). 3-Cyanopyridine (43 mg, 0.4 mmol) and sodium dicyanamide (36 mg, 0.4 mmol) were mixed in a CH_3CN/H_2O solution (20 mL), to which an aqueous solution (8 mL) of $CuCl_2\cdot 2H_2O$ (35 mg, 0.2 mmol) was slowly added with vigorous stirring. A small amount of blue precipitate was formed which was then dissolved by adding additional water (10 mL). The light-blue filtrate was allowed to stand at room temperature, and light-blue needle single crystals suitable for X-ray diffraction were obtained by evaporation of the solvents within 1 week in 65% yield. Anal. Calcd for $C_{16}H_8CuN_{10}$: C, 47.59; H, 2.00; N, 34.68%. Found: C, 47.50; H, 1.98; N, 34.81%. IR (cm^{-1}): 3047*m*, 2300*vs*, 2247*vs*, 2177*vs*, 1601*m*, 1475*m*, 1421*s*, 1354*vs*, 1202*m*, 1125*w*, 1064*w*, 938*w*, 813*w*, 691*s*, 659*m*, 526*m*.

Synthesis of $[Cu(dca)_2(pyom)]_n$ (3). A methanol solution (10 mL) of $Cu(OAc)_2\cdot H_2O$ (40 mg, 0.2 mmol) was added dropwise to a CH_3OH/H_2O solution (20 mL) containing sodium dicyanamide (35 mg, 0.4 mmol) and 2-cyanopyridine (42 mg, 0.4 mmol). A blue solution formed on addition of metal salt to the ligands. The mixture was heated for ca. 30 min with stirring and then filtered after cooling to room temperature. Well-shaped blue block crystals of **3** suitable for X-ray diffraction were obtained within 1 week in 75% yield upon slow evaporation of the solvents. Anal. Calcd for $C_{11}H_8CuN_8O$: C, 39.82; H, 2.43; N, 33.76%. Found: C, 39.62; H, 2.17; N, 33.64%. IR (cm^{-1}): 3188*m*, 3071*w*, 3037*w*, 2297*s*, 2242*s*, 2168*vs*, 1655*s*, 1600*s*, 1496*w*, 1444*m*, 1394*s*, 1353*s*, 1306*w*, 1276*w*, 1220*m*, 1206*m*, 1167*m*, 1155*w*, 1111*w*, 1055*w*, 1027*w*, 966*w*, 917*w*, 872*m*, 814*m*, 761*m*, 705*w*, 666*w*, 652*m*.

X-ray Crystallographic Data Collections and Refinement. Single-crystal X-ray diffraction measurements of **1** (0.30 × 0.25 × 0.08 mm), **2** (0.28 × 0.20 × 0.09 mm), and **3** (0.34 × 0.30 × 0.25 mm) were carried out with a Bruker Smart 1000 CCD diffractometer equipped with a graphite crystal monochromator situated in the incident beam for data collection at 293(2) K. The lattice parameters were obtained by least-squares refinement of the diffraction data of 886 (for **1**), 752 (for **2**), and 818 (for **3**) reflections, respectively, and data collections were performed with Mo Kα radiation ($\lambda = 0.710\ 73$ Å) by ω scan mode in the range of $2.70 < \theta < 25.01°$ (for **1**), $1.87 < \theta < 26.02°$ (for **2**), and $2.57 < \theta < 26.38°$ (for **3**). There was no evidence of crystal decay during data collection for complexes **1**−**3**. All the measured independent reflections were used in the structural analysis, and semiempirical absorption corrections were applied using the SADABS program. The program SAINT[11] was used for integration of the diffraction profiles. All the structures were solved by direct methods using the SHELXS program of the SHELXTL package and refined

Table 1. Crystal Data and Structure Refinement Parameters for Complexes 1−3

	1	2	3
empirical formula	$C_{16}H_8CuN_{10}$	$C_{16}H_8CuN_{10}$	$C_{11}H_8CuN_8O$
crystal habit	light-blue prism	light-blue needle	blue block
M	403.86	403.86	331.79
crystal system	orthorhombic	monoclinic	monoclinic
space group	$Cmca$	$P2_1/n$	$P2_1/n$
a/Å	7.333(2)	7.3080(6)	10.187(5)
b/Å	18.187(6)	16.8212(13)	12.714(7)
c/Å	13.579(4)	14.3215(11)	10.213(5)
β/deg	90	93.355(2)	98.122(8)
V/Å^3	1811.0(9)	1757.5(2)	1309.5(12)
Z	4	4	4
ρ_{calcd}/g cm^{-3}	1.481	1.526	1.688
μ/cm^{-1}	12.29	12.67	16.84
F(000)	812	812	668
no. of observations	874	3451	2672
R_{int}	0.0304	0.0536	0.0390
R^a	0.0302	0.0389	0.0343
$R_w{}^b$	0.0753	0.0939	0.0763
GOF^c	1.088	1.003	1.021
residuals/e Å^{-3}	0.204, −0.222	0.421, −0.315	0.288, −0.325

^{a} $R = \sum||F_o| - |F_c||/\sum|F_o|$. ^{b} $R_w = [\sum[w(F_o^2 - F_c^2)^2]/\sum w(F_o^2)^2]^{1/2}$. ^{c} GOF $= \{\sum[w(F_o^2 - F_c^2)^2]/(n - p)\}^{1/2}$.

with SHELXL.[12] Cu atoms were located from the E-maps, and other non-hydrogen atoms were located in successive difference Fourier syntheses. The final refinement was performed by full-matrix least-squares methods with anisotropic thermal parameters for all the non-hydrogen atoms on F^2. All the hydrogen atoms were first found in difference electron density maps and then placed in the calculated sites and included in the final refinement in the riding model approximation with displacement parameters derived from the parent atoms to which they were bonded. A summary of the crystallographic data and structure refinements is listed in Table 1.

Results and Discussion

Preparation of Compounds 1−3. Complexes **1**−**3** were obtained as neutral molecular complexes by combination of dca with metal Cu^{II} salt and 4-, 3-, and 2-cyanopyridine, respectively (Scheme 1). Compound **1** could be isolated according to the same synthetic procedure, using $CuCl_2$, $Cu(NO_3)_2$, $Cu(OAc)_2$, $CuSO_4$, or $CuBr_2$ as the source of copper (there exist small differences in the experimental phenomena for each case, especially the color of the reaction solution, and all products were confirmed by IR spectra and elemental analyses and part of them were checked by X-ray diffraction). Similar cases were also observed for complexes **2** and **3**, which indicates that the final products

Table 2. Selective Bond Lengths (Å) and Angles (deg) for Complex 1

Bond Lengths			
Cu(1)−N(1)	2.038(3)	Cu(1)−N(3)	2.179(3)
N(2)−C(6)	1.120(6)	N(3)−C(7)	1.139(4)
N(4)−C(7)	1.313(4)		
Bond Angles			
N(1)−Cu(1)−N(3)	89.76(9)	N(3)^a−Cu(1)−N(3)	89.73(15)
N(1)−Cu(1)−N(3)^b	90.24(9)	N(3)−Cu(1)−N(3)^b	90.27(15)
N(2)−C(6)−C(3)	178.9(6)	N(3)−C(7)−N(4)	176.7(3)

^{a} Symmetry code: $1 - x, y, z$. ^{b} Symmetry code: $x, -y + 1, -z$.

are independent of the anions of the metal salts. Complexes **1** and **2** have ligand/dca/Cu^{II} = 2:2:1 ratios and similar chain topology, while **3** is a 1:2:1 coordination polymer containing a single $\mu_{1,5}$-dca bridge. In these specific self-assembled processes, the products **1**−**3** do not depend on the ligand-to-metal ratio (the results were confirmed by IR spectra and elemental analyses). However, altering the metal-to-ligand ratio or the source of Cu^{II} salt in these reactions did lead to differences in the yield and crystal quality. In complexes **1** and **2**, the cyanopyridine molecules behave as monodentate terminal ligands using their pyridyl-nitrogen donors as expected. However, the reaction of 2-cyanopyridine and Cu^{II} in methanol solution leads to the formation of complex **3** containing *O*-methyl picolinimidate as the chelate ligand and no base catalyst (such as sodium methoxide, sodium hydroxide, or various amines) was needed, which was also observed in the previous study.[13a] A reasonable explanation is that the coordination of the Cu^{II} ion activates the C≡N triple bond and makes it much more amenable toward nucleophilic addition by CH_3OH molecules.[13]

X-ray Single-Crystal Structures of Complexes 1−3. (a) Structure Descriptions of $[Cu(dca)_2(4\text{-cypy})_2]_n$ (1) and $[Cu(dca)_2(3\text{-cypy})_2]_n$ (2). The structures of **1** and **2** consist of 1-D neutral polymeric chains of the type commonly found in dca chemistry.[7] Important bond lengths and angles for **1** and **2** are listed in Tables 2 and 3, respectively. For **1** the octahedral copper atom lies on a point of 2/m symmetry and is coordinated to four $\mu_{1,5}$-dca anions, coordinating via the nitrile nitrogen atoms, and two *trans*-4-cyanopyridine (4-cypy) ligands, coordinating via the pyridyl-nitrogen donors, as depicted in Figure 1a. All ligands lie on mirror planes. The Cu^{II} ions show Jahn−Teller contraction (CuN_6), with the two trans Cu−$N_{pyridyl}$ distances (2.038(3) Å) being shorter than the four Cu−N_{dca} distances (2.179-

Scheme 1

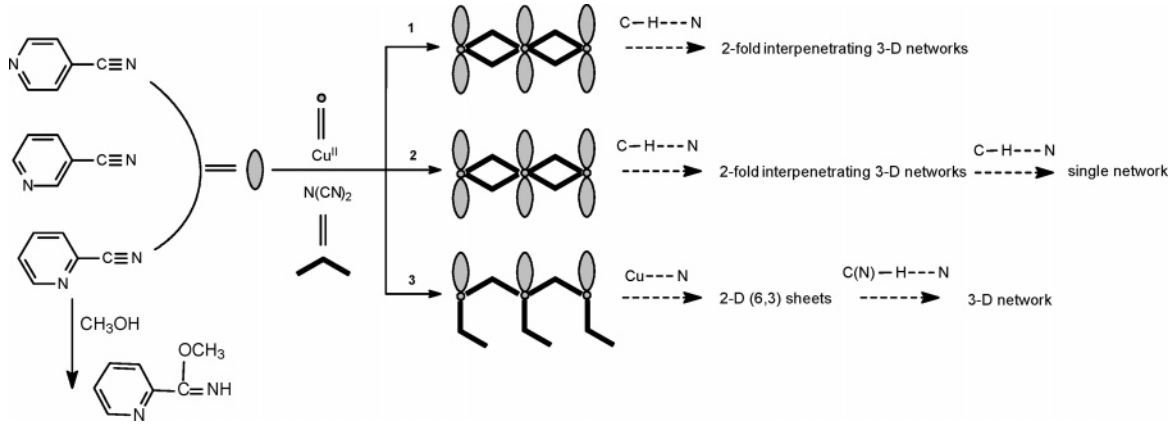

Table 3. Selective Bond Lengths (Å) and Angles (deg) for Complex 2

Bond Lengths			
Cu(1)−N(8)	1.968(3)	Cu(1)−N(1)	2.042(3)
Cu(1)−N(3)	2.047(3)	Cu(1)−N(5)	2.465(4)
Cu(1)−N(7)[a]	1.971(3)	Cu(1)−N(10)[a]	2.419(3)
C(6)−N(2)	1.130(4)	C(12)−N(4)	1.134(4)
C(13)−N(5)	1.149(4)	C(13)−N(6)	1.304(5)
C(14)−N(7)	1.149(4)	C(14)−N(6)	1.292(4)
C(15)−N(8)	1.149(4)	C(15)−N(9)	1.295(4)
C(16)−N(10)	1.141(4)	C(16)−N(9)	1.303(5)
Bond Angles			
N(8)−Cu(1)−N(7)[a]	179.65(13)	N(8)−Cu(1)−N(1)	90.37(11)
N(7)[a]−Cu(1)−N(1)	89.53(11)	N(8)−Cu(1)−N(3)	89.23(11)
N(7)[a]−Cu(1)−N(3)	90.86(11)	N(1)−Cu(1)−N(3)	179.16(11)
N(8)−Cu(1)−N(10)[a]	89.22(12)	N(7)[a]−Cu(1)−N(10)[a]	91.11(12)
N(1)−Cu(1)−N(10)[a]	91.25(11)	N(3)−Cu(1)−N(10)[a]	89.49(10)
N(8)−Cu(1)−N(5)	91.82(12)	N(7)[a]−Cu(1)−N(5)	87.84(12)
N(1)−Cu(1)−N(5)	89.42(11)	N(3)−Cu(1)−N(5)	89.85(11)
N(10)[a]−Cu(1)−N(5)	178.76(12)		

[a] Symmetry code: $x - 1, y, z$.

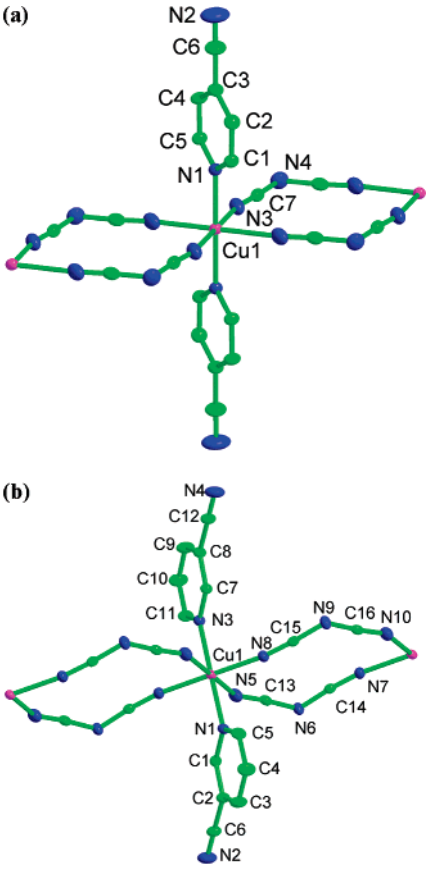

Figure 1. Coordination sphere for the Cu^{II} center in (a) **1** and (b) **2** with atom labeling of the asymmetric unit (hydrogen atoms are omitted for clarity). Thermal ellipsoids are drawn at the 30% level.

(3) Å). The *cis*-N−Cu−N′ bond angles deviate only slightly from O_h symmetry and range from 89.73(15)° to 90.27(15)°. As expected, the dca anions do not coordinate linearly to the metal center, exhibiting a C(7)−N(3)−Cu angle of 162.8(3)°. As shown in Figure 2a, the dca anions connect the metal atoms via the end-to-end bridging mode, producing linear 1-D chains via double dca bridges (Cu···Cu separation within each chain = a = 7.333(2) Å). The shortest Cu···Cu distance between the adjacent chains is 7.716(3) Å. These coordination chains interdigitate to form corrugated

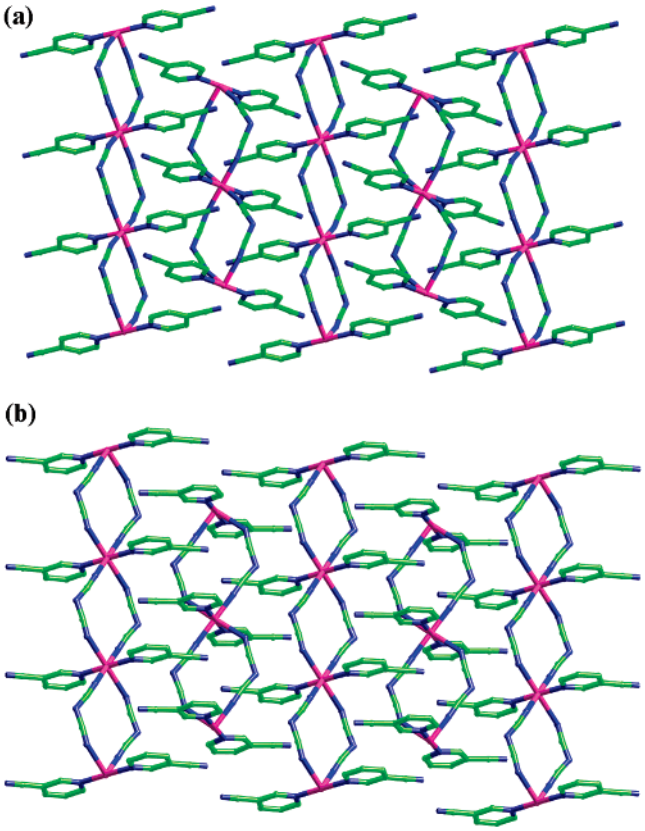

Figure 2. Interdigitated 1-D coordination chains in the structure of (a) **1** and (b) **2**.

Ⓦ 3-D rotatable images of the structures in Ⓦ panel a and Ⓦ panel b are available in PDB format.

layers in which the 4-cypy ligands overlap. The interplanar distance (a/2 = 3.67 Å) is, however, somewhat large to assign significant aromatic stacking interactions. For **2** (Figure 1b), all atoms lie on general positions. The copper atoms are again coordinated to four $\mu_{1,5}$-dca anions and to two pyridyl-bound *trans*-3-cyanopyridine (3-cypy) ligands, and 1-D chains analogous to **1** are formed. The shortest intrachain and interchain Cu···Cu separations are 7.3080(6) Å (=a) and 7.846(5) Å, respectively. The copper atoms in **2**, however, show Jahn−Teller elongation, with two of the $Cu-N_{dca}$ bonds (2.419(3) and 2.465(4) Å) substantially longer than the other two (1.971(3) and 1.968(3) Å), as well as the two $Cu-N_{pyridyl}$ bonds (2.042(3) and 2.047(3) Å). The *cis*-N−Cu−N′ bond angles deviate slightly from O_h symmetry and range from 87.84(12)° to 91.82(12)°. As generally observed, the nitrile substituent of the dca ligands does not bind linearly to the metal center, giving respective C(15)−N(8)−Cu, C(13)−N(5)−Cu, C(16)−N(10)−Cu, and C(14)−N(7)−Cu bond angles of 167.9(3), 136.2(3), 139.6(3), and 165.3(3)°. Similar to **1**, the chains again interdigitate to form corrugated layers, with the average interplanar distance between the 3-cypy ligands being ca. 3.64 Å, as illustrated in Figure 2b.

Analysis of the crystal packing of complexes **1** and **2** reveals that in both structures the 1-D coordination chains are cross-linked by hydrogen-bonding interactions between the free nitrile nitrogen atoms of the cypy ligands and hydrogen atoms of the pyridyl rings (in the 2-position for **1** and in the 4-position for **2**) from

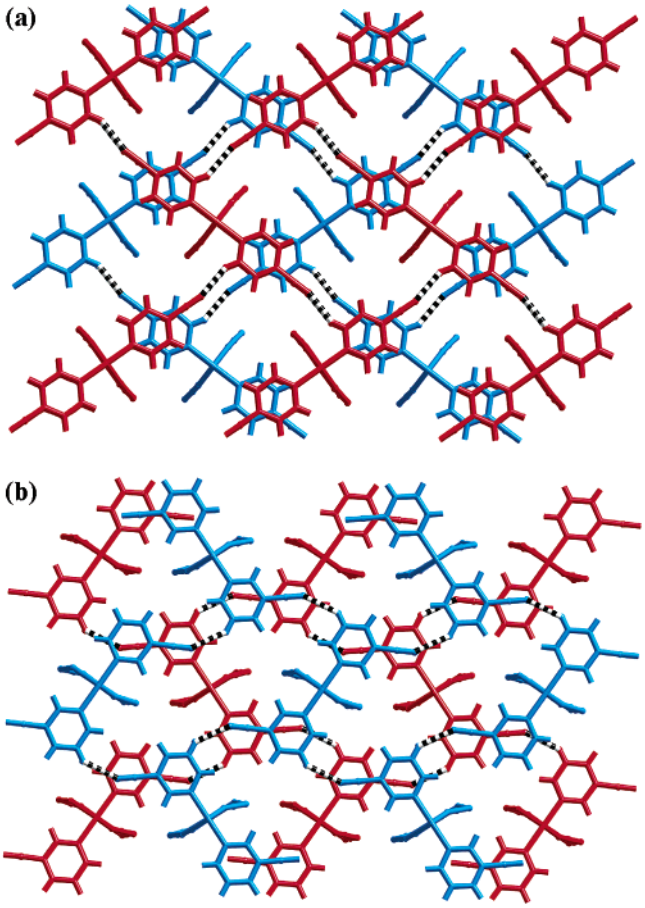

Figure 3. Two interpenetrating hydrogen-bonded 3-D nets in the structure of (a) **1** and (b) **2**. Striped bonds represent the hydrogen bonds, and the two nets are colored differently for clarity.

Ⓦ 3-D rotatable images of the structures in Ⓦ panel a and Ⓦ panel b are available in PDB format.

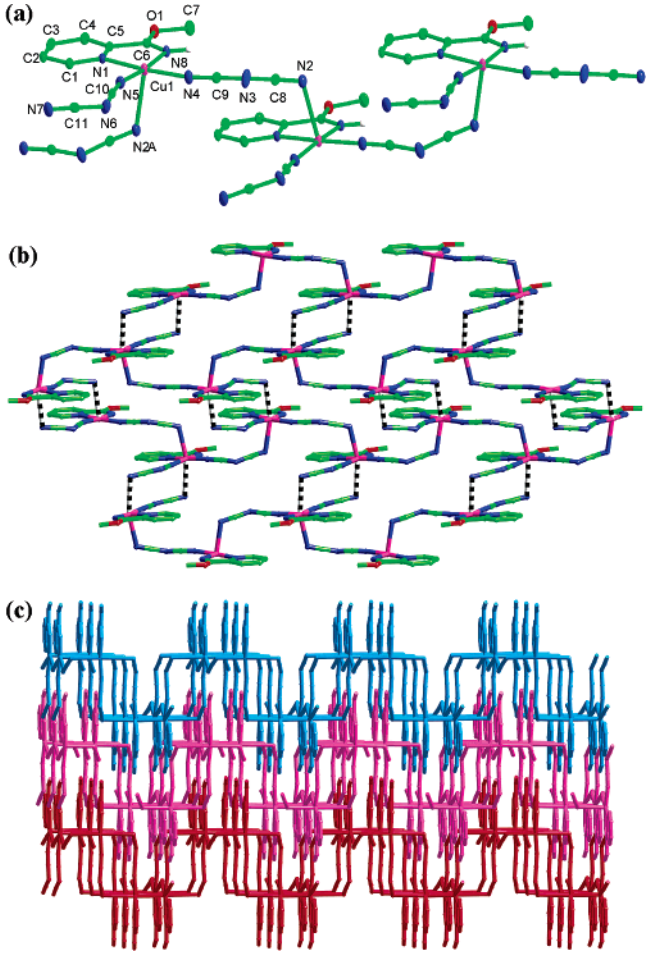

Figure 4. The structure of **3**: (a) 1-D chain bridged by a single dca anion; (b) cross-linking of the 1-D chains by weak Cu–N interactions (striped bonds) to generate a (6,3) sheet; and (c) interdigitation of the highly corrugated sheets.

Ⓦ 3-D rotatable images of the structures in Ⓦ panel b and Ⓦ panel c are available in PDB format.

adjoining chains [**1**: C(1)–H(1)···N(2)^{i} ($i = -x + 1, -y + 1.5, z - 0.5$); **2**: C(4)–H(4A)···N(4)^{i} ($i = -x + 0.5, y + 0.5, -z + 0.5$) and C(10)–H(10A)···N(2)^{ii} ($ii = -x + 0.5, y - 0.5, -z + 1.5$)]. The hydrogen-bonding geometries are as follows: H···N distances of 2.369, 2.531, and 2.520 Å; C···N separations of 3.220, 3.310, and 3.293 Å; C–H···N angles of 151.9, 141.5, and 140.8°, all being in the normal range of such weak interactions.[14] Zigzag hydrogen-bonded chains of cypy ligands running parallel to the z axis are thus formed which are significantly more undulating in **1**. For **1**, these C–H···N weak interactions create two interpenetrating 3-D networks, as depicted in Figure 3a. If each [Cu(4-cypy)$_2$] unit is treated as a single node, then the network topology[15] could be considered as α-Po, with each node connected to six others via four hydrogen bonds (two per 4-cypy, one as donor and the other as acceptor) and two coordination links of (dca)$_2$ bridges. An alternative description of this network would have both 6-connecting nodes (Cu^{II}) and 3-connecting nodes (4-cypy); however, this is a more complicated topology. For **2**, there are also further, weaker hydrogen-bonding interactions between the amide nitrogen atoms of the dca anions and the hydrogen atoms in the 2-position of 3-cypy [C(1)–H(1A)···N(9)^{iii} ($iii = x - 0.5, -y + 0.5, z + 0.5$) and C(7)–H(7A)···N(6)^{iv} ($iv = x - 0.5, -y + 0.5, -z + 0.5$)]. These interactions are not shown in the figure and further connect the two nets into a single network. The C···N separations are 3.517 and 3.494 Å, with H···N distances of 2.633 and 2.617 Å and bond angles of 159.0 and 157.4°, also being in the normal range of such weak interactions.[14]

(b) Structure Description of [Cu(dca)$_2$(pyom)]$_n$ (3). The structure of **3** reveals the decomposition of the 2-cyanopyridine via addition of methanol across the C≡N triple bond, to form a chelating ligand *O*-methyl picolinimidate (C_5H_4N–C(OMe)=NH) (Figure 4a). All atoms lie on general positions. The copper atoms are coordinated to one chelating ligand, coordinating via the pyridyl nitrogen donor (Cu–N = 2.015(2) Å) and the imine nitrogen atom (Cu–N = 1.962(2) Å), two bridging $\mu_{1,5}$-dca anions (Cu–N = 1.948(3) and 2.545(3) Å), and one "terminal" dca anion (Cu–N = 1.965(3) Å). The coordination geometry of the Cu^{II} center (CuN_5) can be described as an almost perfect square pyramid, which is reflected by the τ value (0.026) defined by Addison et al. ($\tau = 0$ for an ideal square pyramid, and $\tau = 1$ for an ideal trigonal bipyramid).[16] The Cu^{II} ion is only 0.101 Å above the basal least-squares plane defined by N(1), N(5), N(4), and N(8) toward the apical site. Similar to **1** and **2**, the dca anions adopt nonlinear bonding

Table 4. Selective Bond Lengths (Å) and Angles (deg) for Complex 3

Bond Lengths			
Cu(1)−N(4)	1.948(3)	Cu(1)−N(8)	1.962(2)
Cu(1)−N(5)	1.965(2)	Cu(1)−N(1)	2.015(2)
Cu(1)−N(2)[a]	2.545(3)	N(8)−C(6)	1.252(3)
O(1)−C(6)	1.323(3)	O(1)−C(7)	1.436(3)
N(2)−C(8)	1.136(4)	N(3)−C(9)	1.281(4)
N(3)−C(8)	1.299(4)	N(4)−C(9)	1.133(3)
N(5)−C(10)	1.141(3)	N(6)−C(10)	1.291(3)
N(6)−C(11)	1.315(4)	N(7)−C(11)	1.139(3)
Bond Angles			
N(4)−Cu(1)−N(8)	91.42(10)	N(4)−Cu(1)−N(5)	91.23(10)
N(8)−Cu(1)−N(5)	173.70(10)	N(4)−Cu(1)−N(1)	172.16(8)
N(8)−Cu(1)−N(1)	80.77(9)	N(5)−Cu(1)−N(1)	96.46(10)
N(4)−Cu(1)−N(2)[a]	96.85(10)	N(5)−Cu(1)−N(2)[a]	89.16(10)
N(8)−Cu(1)−N(2)[a]	96.21(10)	N(1)−Cu(1)−N(2)[a]	84.83(10)

[a] Symmetry code: $0.5 + x$, $0.5 - y$, $0.5 + z$.

configurations about the Cu ion with C(9)−N(4)−Cu = 167.4(2)°, C(10)−N(5)−Cu = 166.5(2)°, and C(8)−N(2)−Cu = 113.5(2)°. Selected bond distances and angles for **3** are listed in Table 4. The bridging dca anions extend the Cu^{II} centers to generate 1-D chains with single dca bridges (Figure 4a). The shortest intrachain and interchain Cu···Cu separations are 7.352(4) and 5.220(4) Å, respectively. These 1-D chains are further cross-linked by weak Cu−N interactions (2.920(3) Å) between the copper atoms and the "uncoordinated" nitrile nitrogen atoms of the terminal dca anions, to form double dca bridges (Cu···Cu = 7.217(6) Å). These weak interactions generate 2-D sheets with (6,3) topology,[15] as shown in Figure 4b, and occur trans to the long Cu−N bond (2.545(3) Å), giving a pseudo Jahn−Teller elongated octahedral geometry for the copper atoms.

Analysis of the crystal packing of **3** indicates that the sheets are highly corrugated and interdigitated (Figure 4c). As a result, there exist hydrogen-bonding interactions which connect the adjoining sheets. These are between the ligand imine group and the uncoordinated nitrile nitrogen of the "monodentate" dca anions [N(8)−H(8)···N(7)^{i} ($i = x, y, z + 1$)] and between the hydrogen in the 3-position of the aromatic ring and the amide nitrogen of the bidentate dca anion [C(4)−H(4)···N(3)^{ii} ($ii = x - 1, y, z$)]. There is also an intrasheet C(2)−H(2)···N(2)^{iii} ($iii = x - 1, y, z - 1$) hydrogen bond between the hydrogen in the 5-position of the aromatic ring and the nitrile nitrogen of the bidentate dca anion which makes the long 2.545(3) Å bond to copper. All the hydrogen-bonding geometries are in the normal range of such weak interactions:[14] H···N distances of 2.176, 2.445, and 2.444 Å; N(C)···N separations of 3.024, 3.369, and 3.346 Å; bond angles of 168.7, 172.4, and 163.5°.

ESR Spectra of Complexes 1−3. ESR powder-spectra of **1**, **2**, and **3** (X-band) have been recorded at variable temperatures. With the exception of the intensity, the shape and g values of ESR results almost do not vary with temperature, as expected. For **1**, only one asymmetric and broad band is observed at low temperature (Figure 5a), which becomes more symmetric when increasing the temperature. In this case, it is necessary to make a simulation which gives $g_x = g_y = 2.12$ and $g_z = 2.18$. For **2**, the typical pattern (Figure 5b) for an elongated O_h geometry of a quasi-isolated Cu^{II} ion is shown: $g_x = g_y = 2.05$ and $g_z = 2.21$. The average of these values is $g = 2.10$, which is exactly the average value obtained by magnetic measurements (see below).

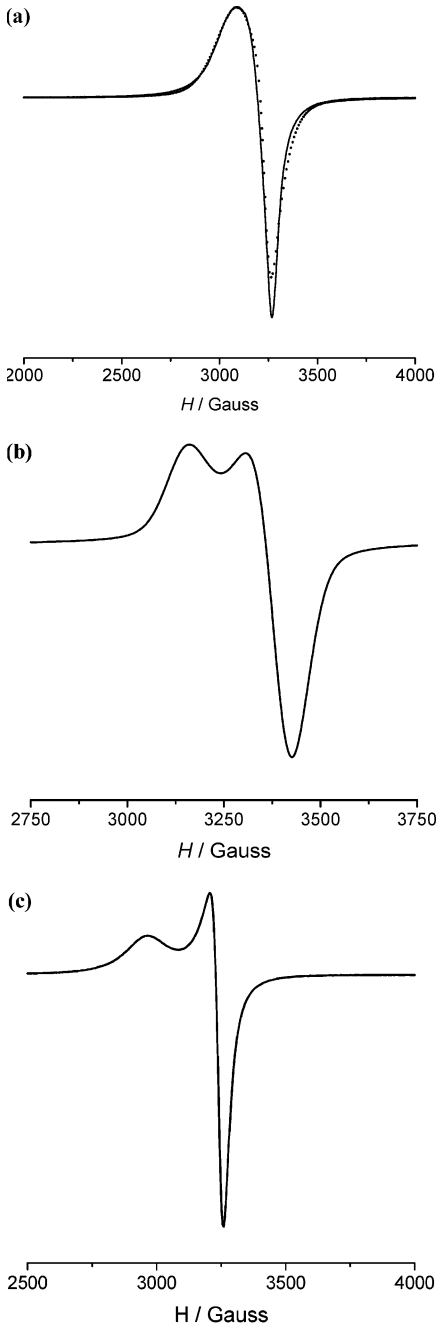

Figure 5. ESR spectra at low temperature (4 K): (a) Complex **1** (solid line). The best simulation is shown as a dotted line (see the text for simulated parameters). (b) Complex **2**. (c) Complex **3**.

Finally, for complex **3**, two bands are observed (Figure 5c) corresponding to the typical anisotropy for a Cu^{II} in square pyramidal geometry: $g_x = g_y = 2.07$ and $g_z = 2.26$. The average of these values is $g = 2.13$, which is exactly the average value obtained by magnetic measurements (see below).

Magnetic Properties of Complexes 1−3. The magnetic properties of complexes **1**, **2**, and **3** are shown in Figure 6a−c, respectively, as χ_M (inset) and $\chi_M T$ vs T plots (χ_M is the molar magnetic susceptibility for one Cu^{II} ion). The values of $\chi_M T$ at 300 K are 0.433 cm^3 mol^{-1} K for **1**, 0.413 cm^3 mol^{-1} K for **2**, and 0.426 cm^3 mol^{-1} K for **3**, which are as expected for one magnetically quasi-isolated spin doublet ($g > 2.00$). Starting

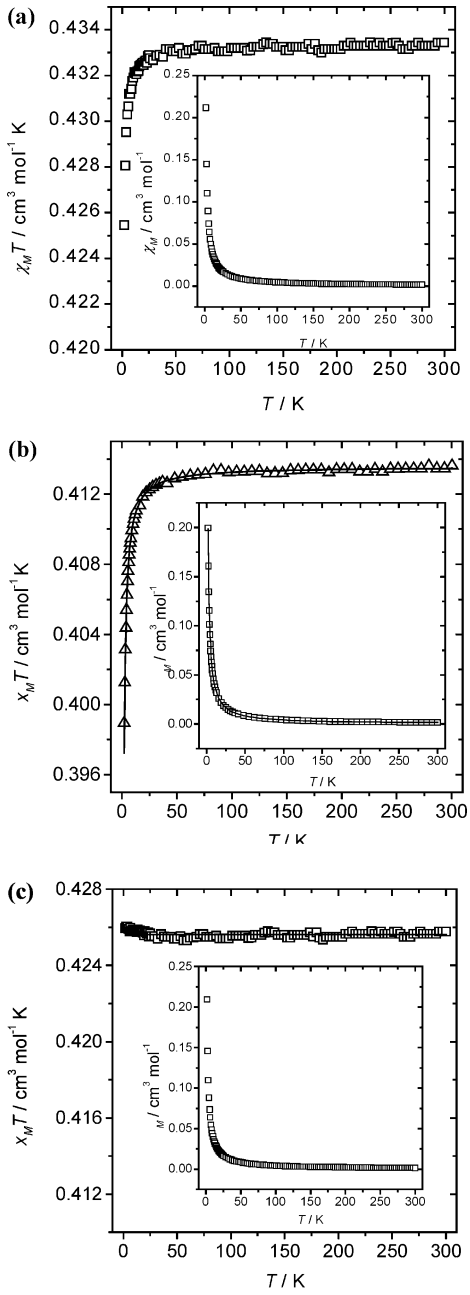

Figure 6. Plot of $\chi_M T$ and χ_M (inset) vs T: (a) Complex **1**. (b) Complex **2**. The solid line represents the best fit (see the text). (c) Complex **3**. The solid line in $\chi_M T$ indicates the Curie law.

from room temperature, the $\chi_M T$ values for **1** are practically constant to 15 K and then smoothly decrease to 0.425 cm^3 mol^{-1} K at 2 K. For **2**, the values do not vary greatly, as anticipated for a Curie-like system, until 50 K where a small downturn is noted and finally attend to 0.399 cm^3 mol^{-1} K at 2 K. They keep practically constant for **3**, apart from a small, but significant, increase at very low temperature (see below). The χ_M curves (Figure 6, inset) start at 0.00144 cm^3 mol^{-1} for **1**, 0.00138 cm^3 mol^{-1} for **2**, and 0.00142 cm^3 mol^{-1} for **3** and increase in a uniform way to 0.21167 cm^3 mol^{-1} for **1**, 0.19948 cm^3 mol^{-1} for **2**, and 0.20913 cm^3 mol^{-1} for **3**, at 2 K, respectively. The global features are characteristic of nil magnetic interaction for **1** and **3** and very weak antiferromagnetic interaction for **2**.

Complexes **1**, **2**, and **3** are actually quasi-isolated Cu^{II} one-dimensional entities. This gives uniform $S = {}^1/_2$ systems with only one value of J. The fits of the magnetic data for **1** and **2** have been carried out with the CLUMAG program,[17] modeling the input with 12 Cu^{II} atoms, which is the typical number taken in these types of Cu^{II} compounds, as it approaches to infinite number. Both cases, like in all one-dimensional systems, have been mathematically cycled, to be as close as possible to a true one-dimensional system. The best-fit parameters obtained with this computing model are $J < -0.01$ cm^{-1} for **1** and $J = -0.11 \pm 0.02$ cm^{-1}, $g = 2.10 \pm 0.01$, and $R = 1.0 \times 10^{-6}$ for **2** (R is the agreement factor defined as $\sum_i[(\chi_M T)_{obs} - (\chi_M T)_{calc}]^2/\sum[(\chi_M T)_{obs}]^2$). These results indicate very small antiferromagnetic coupling through the dca bridging ligands, especially in complex **1**, in which the J value lies in the experimental error for a simple Curie law for an isolated Cu^{II} ion. Additionally, complex **3** follows the Curie law with a g value of 2.13 (see Figure 6c). However, the final pattern of the $\chi_M T$ curve for **3** at low temperature is not common for this kind of one-dimensional Cu^{II} complex. The tendency of $\chi_M T$ at low temperature is to decrease, owing to the usual weak intermolecular antiferromagnetic interactions. In **3** this tendency is the opposite: $\chi_M T$ values increase, though only weakly.

Magneto-structural Correlations. The small J values calculated for these 1-D systems with $\mu_{1,5}$-dca bridging ligands do not allow accurate magneto-structural correlations to be drawn. The only useful analysis to be made is the comparison of these values with those reported for similar complexes. In Table 5, the main structural parameters for complexes **1**, **2**, and **3** and those reported in the literature are given.[18–24] There are some features that can be highlighted as follows: (a) the J value is always very small or nil, and except in one case this weak coupling is antiferromagnetic; (b) when there are two dicyanamide bridging ligands between the Cu^{II} ions, these centers show a distorted octahedral environment (Jahn–Teller effect), and almost all complexes do not have magnetic coupling ($J \gg 0$ cm^{-1}) within experimental error; (c) when there is only one dicyanamide bridging ligand between the Cu^{II} ions, these ions are pentacoordinated, and a large variety of J values (from -0.44 to $+0.2$ cm^{-1}) are observed.

From magnetic point of view, it is important to underline that the linkage between Cu^{II} ions through the dca bridging ligands can be equatorial–equatorial (usually short–short) or equatorial–axial (short–long). When the coordination mode is equatorial–equatorial, the weak coupling across this extended bridge can be understood as follows: the magnetic orbital describing the unpaired electron on a Cu^{II} ion in square-pyramidal or elongated distorted octahedral geometries is of the $d_{x^2-y^2}$ type (the x and y axes being roughly defined by the short equatorial bonds). The overlap between two of these orbitals through the polyatomic $\mu_{1,5}$-dca bridge is expected to be very weak, and consequently, the antiferromagnetic coupling, which is proportional to the square of this overlap, is predicted to be a weak one, as observed. A typical example of this short–short (equatorial–equatorial) coordination is $[Cu(pyim)(H_2O)(\mu\text{-dca})]_n(NO_3)_n$,[19] in which the J value is small but antiferromagnetic (-0.35 cm^{-1}) (Table 5).

For the equatorial–axial coordination mode, it is possible to obtain weak antiferro- or ferromagnetic

Table 5. Comparison of the Structural and Magnetic Parameters for $\mu_{1,5}$-Dicyanamide Cu^{II} Complexes (without Other Bridging Ligands)

compound[a]	n[b]	Cu^{II} geometry	Cu−N_{dca} (Å)	J (cm^{-1})	refs
$[Cu(pym)_2(\mu\text{-dca})_2]$	2	O_h (elongated)	1.995 and 2.425	≈0	18
$[Cu(bpa)(\mu\text{-dca})]$[c]	2	O_h (elongated)	2.001 and 2.467	−0.22	19
$[Cu(ampym)_2(\mu\text{-dca})_2]$	2	O_h (elongated)	1.972 and 2.416	≈0	20
$[Cu(4\text{-cypy})_2(\mu\text{-dca})_2]_n$	2	O_h (contraction)	2.179 and 2.179	≈0	this work
$[Cu(3\text{-cypy})_2(\mu\text{-dca})_2]_n$	2	O_h (elongated)	1.971 and 1.968 2.419 and 2.465	−0.11	this work
$[Cu(pyim)(H_2O)(\mu\text{-dca})]_n(NO_3)_n$	1	*sp* ($\tau = 0.037$)	1.964 and 1.979	−0.35	19
$[Cu(dpa)(\mu\text{-dca})]_n$	1	*sp* ($\tau = 0.38$)	2.012 and 2.175	−0.10	19
$[Cu(dmbipy)(\mu\text{-dca})_2]_n$	1	*sp* ($\tau = 0.21$)	2.247 and 1.984	≈0	21
$[Cu(bpy)(\mu\text{-dca})_2]_n$	1	*sp* ($\tau = 0.30$)	1.996 and 2.167	≈0	22
$[Cu(phen)(\mu\text{-dca})_2]_n$	1	*sp* ($\tau = 0.12$)	2.008 and 2.287	+0.2	22, 23
$[Cu_2L_2(\mu\text{-dca})_2(ClO_4)_2]_2$	1	sp ($\tau = 0.12$) *bpt* ($\tau = 0.72$)	1.959 and 2.002 2.026 and 2.011	−0.44	24
$[Cu(dca)_2(pyom)_2]_n$	1	*sp* ($\tau = 0.03$)	1.948 and 2.545	≈0	this work

[a] Pym = pyrimidine; bpa = 1,2-bis(4-pyridyl)ethane; ampym = 2-aminopyrimidine; pyim = 2-(2-pyridyl)imidazole; dpa = 2,2′-dipyriylamine; dmbipy = 5,5′-dimethyl-2,2′-bipyridine; bpy = 2,2′-bipyridine; phen = 1,10-phenantroline; L = 1,5,9-triazacyclododecane. [b] n = number of $\mu_{1,5}$-dicyanamide ligands. [c] Bpa also acts as bridging ligand; however, according to the authors it does not create any magnetic coupling.

coupling. For example, a good explanation of the ferromagnetic coupling in $[Cu(phen)(\mu\text{-dca})_2]_n$ has been given by Julve et al.:[22] the weak ferromagnetic interaction corresponds to a case of accidental orthogonality analogous to that observed in other cases where the out-of-plane exchange pathway is operative, through either monatomic (μ-chloro) or polyatomic (μ-carboxylato) paths. This accidental orthogonality between the magnetic orbitals is strongly dependent on structural features, and even slight structural modifications can destroy it. The τ parameter for that complex is only 0.13, which indicates a good percentage of pure square-pyramidal geometry and a short−long (equatorial−apical) magnetic pathway. Complex **3** is a similar but slightly different case: the τ parameter is one of the smallest ($\tau = 0.03$; Table 5), which would favor the ferromagnetic coupling, but the Cu−N apical distance is very long (2.545 Å), thus avoiding the possible ferromagnetic coupling, as expected from the explanation of Julve et al. in their similar complex.[22] In any case, as indicated above, from Figure 6c it could be deduced that $\chi_M T$ values increase at very low temperature, when normally these values tend to decrease. This feature could indicate some very small ferromagnetic coupling, but within the experimental error.

Infrared Spectral Studies. In the IR spectra of complexes **1**−**3**, the absorption bands resulting from the skeletal vibrations of the pyridyl rings appear in the 1400−1600 cm^{-1} region. The dca anion of $NaN(CN)_2$ exhibits three sharp and strong characteristic stretch frequencies attributed to $\nu_{as} + \nu_s$(C−N) combination modes (2286 cm^{-1}), ν_{as}(C≡N) (2232 cm^{-1}), and ν_s(C≡N) (2179 cm^{-1}), respectively.[25] The IR spectra of complexes **1**−**3** show strong absorption in the 2300−2168 cm^{-1} region corresponding to ν_{CN} of dca: for **1**, 2290 cm^{-1} [$\nu_{as} + \nu_s$(C−N)], 2244 cm^{-1} [ν_{as}(C≡N)], and 2176 cm^{-1} [ν_s(C≡N)]; for **2**, 2300 cm^{-1} [$\nu_{as} + \nu_s$(C−N)], 2247 cm^{-1} [ν_{as}(C≡N)], and 2177 cm^{-1} [ν_s(C≡N)]; for **3**, 2297 cm^{-1} [$\nu_{as} + \nu_s$(C−N)], 2242 cm^{-1} [ν_{as}(C≡N)], and 2168 cm^{-1} [ν_s(C≡N)]. The shifts toward higher frequencies of these peaks as compared to those of free dca are due to the bridging modes of dca in these complexes. Furthermore, all dca anions adopt the same $\mu_{1,5}$-binding mode in **1**−**3** and this analogy between the dca bridges accounts for their practically identical frequency values as listed above. Additionally, the absorption bands of the ν_{as}(C−N) stretching frequencies (1400−1300 cm^{-1}) and the ν_s(C−N) stretch (950−900 cm^{-1}) are also observed in the spectra: 1332 and 942 cm^{-1} for **1**, 1354 and 938 cm^{-1} for **2**, and 1353 and 917 cm^{-1} for **3**. These vibrations occur in the range found for other related $\mu_{1,5}$-dca Cu^{II} complexes.[19,26] Another notable feature is that the spectrum of compound **3** has a sharp band with medium intensity at 3188 cm^{-1}, characteristic of the N−H vibration of *O*-methyl picolinimidate.

Thermogravimetric Analysis. Complexes **1**−**3** are air stable and can retain their structural integrity at room temperature for a considerable length of time. Thermogravimetric analyses were conducted to determine the thermal stability of these materials. For **1**, the first weight loss of 51.56% from 135 to 290 °C (peak: 180 °C) corresponds to the loss of two 4-cyanopyridine molecules (calculated: 51.08%). The remaining substance does not lose weight upon further heating until a weight loss occurs in the 320−700 °C region (peak: 631 °C), corresponding to the removal of two dca ligands (observed: 33.12%; calculated: 32.70%). Further heating to 900 °C of the sample indicates no weight loss. For **2**, the first weight loss of 39.02% from 110 to 180 °C (peak: 165 °C) corresponds to the release of one and a half 3-cyanopyridine molecules (calculated: 38.67%). The remaining moiety does not lose weight upon further heating until two consecutive weight losses occur in the 200−660 °C region (peak: 335 and 617 °C; total weight: 45.02%), corresponding to the removal of half of a 3-cyanopyridine and two dca ligands (calculated: 45.59%). Just like **1**, further heating to 900 °C of the sample reveals no weight loss. For **3**, the TGA curve is more complicated. The coordination framework remains intact until three consecutive weight losses occur in the 200−800 °C region (peak: 209, 397, and 715 °C; total weight: 61.84%). Further heating to 900 °C of the sample also indicates a continuous and slow weight loss.

Conclusions and Remarks

In the present study, we have further demonstrated the assembly of supramolecular architectures from low to higher dimensionality via the interplay of both coordinative and hydrogen-bonding interactions, based

on the combined use of dca and terminal cypy ligands and Cu^{II} ions. We are currently extending this strategy by using other similar terminal ligands with coordinate-negative groups as the hydrogen-bonding acceptors to construct new supramolecular networks. Furthermore, this work also allows us (a) to prepare and characterize three double (**1** and **2**) or single (**3**) dca-bridged coordination chains with dca exhibiting the end-to-end bridging mode and (b) to check and compare the efficiency of this coordination mode of dca in mediating exchange interactions between Cu^{II} ions with different coordination environments.

Acknowledgment. This work was financially supported by the National Natural Science Foundation of China (No. 20401012) and the Key Project of Tianjin Natural Science Foundation. S.R.B. acknowledges the financial support from the Australian Research Council, and J.R. that from the Spain Government (Grant BQU2003/00539).

Supporting Information Available: Crystallographic information files (CIF) of complexes **1**–**3**. This material is available free of charge via the Internet at http://pubs.acs.org.

References

(1) (a) Desiraju, G. R. *Angew. Chem., Int. Ed. Engl.* **1995**, *34*, 2311. (b) Aakeröy, C. B.; Beatty, A. M. *Aust. J. Chem.* **2001**, *54*, 409. (c) Holman, K. T.; Pivovar, A. M.; Swift, J. A.; Ward, M. D. *Acc. Chem. Res.* **2001**, *34*, 107. (d) Burrows, A. D. *Struct. Bonding* **2004**, *108*, 55. (e) Braga, D.; Maini, L.; Polito, M.; Grepioni, F. *Struct. Bonding* **2004**, *111*, 1.

(2) (a) Batten, S. R.; Robson, R. *Angew. Chem., Int. Ed.* **1998**, *37*, 1460. (b) Blake, A. J.; Champness, N. R.; Hubberstey, P.; Li, W. S.; Withersby, M. A.; Schröder, M. *Coord. Chem. Rev.* **1999**, *183*, 117. (c) Moulton, B.; Zaworotko, M. J. *Chem. Rev.* **2001**, *101*, 1629. (d) Carlucci, L.; Ciani, G.; Proserpio, D. M. *Coord. Chem. Rev.* **2003**, *246*, 247. (e) Janiak, C. *Dalton Trans.* **2003**, 2781.

(3) (a) Robson, R. *J. Chem. Soc., Dalton Trans.* **2000**, 3735. (b) Kitagawa, S.; Masaoka, S. *Coord. Chem. Rev.* **2003**, *246*, 73. (c) Biradha, K. *CrystEngComm* **2003**, *5*, 374. (d) Beatty, A. M. *Coord. Chem. Rev.* **2003**, *246*, 131. (e) Rao, C. N. R.; Natarajan, S.; Vaidhyanathan, R. *Angew. Chem., Int. Ed.* **2004**, *43*, 1466.

(4) (a) Hagrman, P. J.; Hagrman, D.; Zubieta, J. *Angew. Chem., Int. Ed.* **1999**, *38*, 2639. (b) Kahn, O. *Acc. Chem. Res.* **2000**, *33*, 647. (c) Evans, O. R.; Lin, W. *Acc. Chem. Res.* **2002**, *35*, 511. (d) Yaghi, O. M.; O'Keeffe, M.; Ockwig, N. W.; Chae, H. K.; Eddaoudi, M.; Kim, J. *Nature* **2003**, *423*, 705. (e) Kesanli, B.; Lin, W. *Coord. Chem. Rev.* **2003**, *246*, 305. (f) Kitagawa, S.; Kitaura, R.; Noro, S. *Angew. Chem., Int. Ed.* **2004**, *43*, 2334.

(5) (a) Batten, S. R.; Jensen, P.; Moubaraki, B.; Murray, K. S.; Robson, R. *Chem. Commun.* **1998**, 439. (b) Kurmoo, M.; Kepert, C. J. *New J. Chem.* **1998**, *22*, 1515. (c) Manson, J. L.; Kmety, C. R.; Huang, Q.-Z.; Lynn, J. W.; Bendele, G. M.; Pagola, S.; Stephens, P. W.; Liable-Sands, L. M.; Rheingold, A. L.; Epstein, P. W.; Miller, J. S. *Chem. Mater.* **1998**, *10*, 2552. (d) Jensen, P.; Batten, S. R.; Fallon, G. D.; Moubaraki, B.; Murray, K. S.; Price, D. J. *Chem. Commun.* **1999**, 177. (e) Batten, S. R.; Jensen, P.; Kepert, C. J.; Kurmoo, M.; Moubaraki, B.; Murray, K. S.; Price, D. J. *J. Chem. Soc., Dalton Trans.* **1999**, 2987. (f) Manson, J. L.; Kmety, C. R.; Epstein, A. J.; Miller, J. S. *Inorg. Chem.* **1999**, *38*, 2552.

(6) (a) Cho, J.; Lee, U.; Kim, J. C. *Transition Met. Chem.* **2002**, *27*, 429. (b) Bessler, K. E.; Romualdo, L. L.; Salviano, P. D.; Deflon, V. M.; Maichle-Mossmer, C. *Z. Anorg. Allg. Chem.* **2001**, *627*, 651. (c) Kuang, S.-M.; Fanwick, P. E.; Walton, R. A. *Inorg. Chem.* **2001**, *40*, 5682. (d) Brezina, F.; Travnicek, Z.; Sindelar, Z.; Pastorek, R.; Marek, J. *Transition Met. Chem.* **1999**, *24*, 459. (e) Zhang, L. Y.; Shi, L. X.; Chen, Z. N. *Inorg. Chem.* **2003**, *42*, 633. (f) Kuang, S.-M.; Fanwick, P. E.; Walton, R. A. *Inorg. Chem.* **2002**, *41*, 147.

(7) Batten, S. R.; Murray, K. S. *Coord. Chem. Rev.* **2003**, *246*, 103.

(8) Brammer, L. *Dalton Trans.* **2003**, 3145.

(9) Roesky, H. W.; Andruh, M. *Coord. Chem. Rev.* **2003**, *236*, 91.

(10) Lin, P.; Henderson, R. A.; Harrington, R. W.; Clegg, W.; Wu, C. D.; Wu, X. T. *Inorg. Chem.* **2004**, *43*, 181.

(11) *SAINT Software Reference Manual*; Bruker AXS: Madison, WI, 1998.

(12) Sheldrick, G. M. *SHELXTL NT Version 5.1. Program for Solution and Refinement of Crystal Structures*; University of Göttingen: Göttingen, Germany, 1997.

(13) (a) Jamnicky, M.; Segl'a, P.; Koman, M. *Polyhedron* **1995**, *14*, 1837 and references therein. (b) Constable, E. C. *Metals and Ligand Reactivity*: *An Introduction to the Organic Chemistry and Metal Complexes*; VCH: Weinheim, 1996.

(14) Desiraju, G. R.; Steiner, T. *The Weak Hydrogen Bond in Structural Chemistry and Biology*; Oxford University Press: Oxford, 1999.

(15) Wells, A. F. *Three-Dimensional Nets and Polyhedra*; Wiley-Interscience: New York, 1977.

(16) Addison, A. W.; Rao, T. N.; Reedijk, J.; Van Rijn, J.; Verschoor, G. C. *J. Chem. Soc., Dalton Trans.* **1984**, 1349.

(17) CLUMAG Program: Gatteschi, D.; Pardi, L. *Gazz. Chim. Ital.* **1993**, *123*, 231. This program uses a full-diagonalization procedure, employing the irreducible tensor operator formalism (ITO).

(18) Manson, J. L.; Gu, J.; Schlueter, J. A.; Wang, H.-H. *Inorg. Chem*. **2003**, *42*, 3950.

(19) Carranza, J.; Brennan, C.; Sletten, J.; Lloret, F.; Julve, M. *J. Chem. Soc., Dalton Trans*. **2002**, 3164.

(20) Jensen, P.; Price, D. J.; Batten, S. R.; Moubaraki, B.; Murray, K. S. *Chem.—Eur. J*. **2000**, *6*, 3186.

(21) Kooijman, H.; Spek, A. L.; van Albada, G. A.; Reedijk, J. *Acta Crystallogr.* **2002**, *C58*, m124.

(22) Vangdal, B.; Carranza, J.; Lloret, F.; Julve, M.; Sletten, J. *J. Chem. Soc., Dalton Trans*. **2002**, 566.

(23) Luo, H. J.; Hong, M. C.; Weng, J. B.; Zhao, J. Y.; Cao, R. *Inorg. Chim. Acta* **2002**, *329*, 59.

(24) Gu, W.; Bian, H.-D.; Xu, J.-Y.; Liu, Z.-Q.; Cheng, P.; Yan, S.-P.; Liao, D.-Z.; Jiang, Z.-H. *Inorg. Chem. Commun*. **2003**, *6*, 966.

(25) Köhler, H.; Kolbe, A.; Lux, G. *Z. Anorg. Allg. Chem.* **1977**, *428*, 103.

(26) van Albada, G. A.; Mutikainen, I.; Turpeinen, U.; Reedijk, J. *Acta Crystallogr.* **2001**, *E57*, m421.

CG0496888